JOURNAL OF CHEMICAL & ENGINEERING DATA

ARTICLE

pubs.acs.org/jced

The Effect of Surface Adsorption and Molecular Geometry on the Determination of Henry's Law Constants for Fluorotelomer Alcohols

Yaoxing Wu[†] and Victor W.-C. Chang*

School of Civil and Environmental Engineering, Nanyang Technological University, 50 Nanyang Avenue, 639798 Singapore

ABSTRACT: Fluorotelomer alcohols (FTOHs) are one important subgroup of perfluorinated compounds (PFCs), yet Henry's law constant (K_H) of FTOHs, which is also known as the air−water partition coefficient, remains poorly understood with a wide range of reported values. This study measured the K_H of FTOHs from (309.6 to 334.2) K using the integrated gas-stripping method (IGS) for the first time, which has a lower surface-to-volume ratio comparing to the headspace method (HS). Two different materials, namely, stainless steel and glass, were chosen for constructing the stripping vessels. Results indicated significantly stronger adsorption of long-chained FTOHs on glass surface, which led to a significant bias in K_H derivation. K_H values extrapolated to 298 K of 4:2, 6:2, 8:2, and 10:2 FTOH, using a stainless steel vessel, showed no linear increase. A similar tendency was also reported by other groups using the HS approach. The unique molecular geometry of FTOHs was suspected to be responsible for the unusual tendency observed and false predications by modeling software including SPARC and EPI Suite. Compared with HS results reported by others, the K_H values obtained in this study were higher. The discrepancy might be mainly due to the different extent of surface adsorption engaged in the two approaches.

INTRODUCTION

Perfluorinated compounds (PFCs) are one group of emerging contaminants characterized by a hydrophobic perfluorinated alkyl chain and a hydrophilic end group with the general structure $F(CF_2)_nR$. The perfluorinated chains n vary in lengths from (4 to 17) with the predominance of linear eight carbons. The strength of the carbon−fluorine bond and shielding effect of fluorine atoms render the strong chemical and thermal stability of PFCs.

Fluorotelomer alcohols (FTOHs) are one of the subgroups of PFCs with the general structure $F(CF_2)_nCH_2CH_2OH$, where n is an even number. The FTOHs are often referred to as X:Y FTOH based upon the number of fluorinated carbon atoms (X) and hydrogenated carbon atoms (Y). These compounds have drawn great attention recently because of their global distribution, environmental persistence, and potential toxicity to humans. FTOHs are often used in the production of fluorotelomer-based substances to provide oil and water repellent properties. The typical application of fluorotelomer-based compounds includes adhesives, cleaning agents, food packaging, fire fighting foams, and so forth. The industry processes in making fluorotelomer-based substances leave unreacted residual FTOHs in the final products with a mass fraction of (0.001 to 0.005).[1−3] It is estimated that at least 10^5 kg of FTOHs is released from the residuals to environment annually and their occurrence in atmosphere has been widely reported in global range including the arctic region.[4−6]

FTOHs could undergo biodegradation and oxidation in the atmosphere to yield a homologous series of perfluorocarboxylic acids (PFCAs), which persist in the environment and accumulate in the body of humans and wildlife.[7] In addition to atmospheric degradation, FTOHs could also be potentially removed from the atmosphere through wet and dry deposition.[8] The estimated half-life of FTOHs in the atmosphere is 20 d which is sufficient to allow for a wide range distribution in the environment.[9]

Henry's law constant (K_H), which describes the equilibrium partitioning between gaseous and aqueous phases, is essential for predicting the environmental behavior, transport, and fate of many classes of organic chemicals.[10] In this study, the K_H is expressed as the ratio of vapor pressure P_g to its aqueous concentration C_w. The K_H can also take the dimensionless form (K_{AW}), which is related to K_H by

$$K_{AW} = \frac{C_A}{C_W} = \frac{K_H}{RT} \quad (1)$$

where C_A is the concentration of the compound in the gas phase; R is the ideal gas constant; and T is the thermodynamic temperature.

The enthalpy ΔH and entropy ΔS of phase change from the dissolved phase to gas phase were calculated using the slope and intercept values by plotting ln K_{AW} against the reciprocal of absolute temperature.

$$\ln K_{AW} = -\frac{\Delta H}{RT} + \frac{\Delta S}{R} \quad (2)$$

where ΔH represents the energy required to overcome the intermolecular interaction in transferring molecules between the two phases. ΔS is the associated entropy change. This expression assumes that ΔH and ΔS are temperature-independent, which is a reasonable assumption over a small temperature range in this study from (309.6 to 334.2) K.

Despite numerous reports on environmental concentrations, toxicological concerns, and treatment methods about PFCs,[11−13] very little experimental information is available on their physicochemical properties.[14] Lei et al.[15] and Goss et al.[16] have used

Received: May 13, 2011
Accepted: June 29, 2011
Published: July 19, 2011

the equilibrium headspace gas chromatography (HS) approach to determine the K_H of 4:2, 6:2, and 8:2 FTOH, which measures the equilibrium headspace concentration in the closed glass vials with typical sizes of (10 or 20) cm^3.[15,16] This approach is relatively reliable and straightforward in the experimental processes. However, the adsorption of 8:2 FTOH to the glass wall at equilibrium might lead to an underestimation of K_H, as reported by Goss et al.[16]

To our knowledge, the current study is the first to employ an integrated gas-stripping method (IGS) to determine K_H of FTOHs. This approach involves the measurement of declining aqueous and air concentration as the water solution is purged with a flow of gas. K_H could be calculated as the ratio of time-integrated gas phase concentration (C_a) over the average of the two aqueous concentrations which were measured at the start ($C_{w(n)}$) and end ($C_{w(n+1)}$) of each air samples.

$$K_{AW} = \frac{C_a}{(C_{w(n)} + C_{w(n+1)})/2} \quad (3)$$

Comparing to small glass vials in the HS method, IGS requires a larger vessel volume, typically in the range of liters, for gas stripping. This leads to a much lower surface-to-volume ratio than that in HS. As the long-chained FTOHs had been reported to have significant surface adsorption, IGS has the advantage to minimize the artifact in this regard. Furthermore, the IGS method allows repeated measurements of K_H in one experimental run, which improves the data quality control.

This study measured K_H values for 4:2, 6:2, 8:2, and 10:2 FTOH from (309.6 to 334.2) K using the IGS method. Surface adsorption, which was suspected as an potential influencing factor to the measurement in IGS, was also investigated by batch experiments employing glass and stainless steel vials. K_H values obtained via IGS in this study were compared with K_H generated by modeling software (EPI Suite and SPARC) and HS approach from references to better understand the molecular geometry of FTOHs, as well as the advantages and potential flaws in these approaches.

EXPERIMENTAL SECTION

Chemicals. Standards of FTOHs including 3,3,4,4,5,5,6,6,6-nonafluorohexan-1-ol (4:2 FTOH, mass fraction purity of 0.97, CAS No.: 2043-47-2), 3,3,4,4,5,5,6,6,7,7,8,8,8-tridecafluorooctan-1-ol (6:2 FTOH, mass fraction purity of 0.97, CAS No.: 647-42-7), 3,3,4,4,5,5,6,6,7,7,8,8,9,9,10,10,10-heptadecafluorodecan-1-ol (8:2 FTOH, mass fraction purity of 0.97, CAS No.: 678-39-7), and 3,3,4,4,5,5,6,6,7,7,8,8,9,9,10,10,11,11,12,12,12-henicosafluorododecan-1-ol (10:2 FTOH, mass fraction purity of 0.96, CAS No.: 865-86-1) were purchased from ABCR, Germany, Sigma-Aldrich, Singapore and Lancaster Synthesis, Singapore. ^{13}C-8:2 FTOH $[m+4]$ with a concentration of $1.35 \cdot 10^{-4}$ mol·kg^{-1} in methanol (surrogate for FTOHs) were from Wellington Laboratories, Canada. Internal standards 2,2,3,3,4,4,5,5,6,6,7,7,8,8,8-pentadecafluorooctan-1-ol (7:1 FA, mass fraction purity of 0.98, CAS No.: 307-30-2) and 2,2,3,3,4,4,5,5,6,6,7,7,8,8,9,9,10,10,11,-11,12,12,12-tricosafluorododecan-1-ol (11:1 FA, mass fraction purity of 0.90, CAS No.: 423-65-4) were from Lancaster Synthesis, Singapore.

Ethyl acetate (ETOAc, for gas chromatography Suprasolv, mass fraction purity ≥ 0.998, CAS No.: 141-78-6) was obtained from Merck, Singapore. 2-Methoxy-2-methylpropane (MTBE, puriss, mass fraction purity ≥ 0.995, CAS No.: 1634-04-4) was from Sigma-Aldrich, Singapore. Propan-2-one (acetone, mass fraction purity ≥ 0.998, CAS No.: 67-64-1) was purchased from Fisher Scientific, UK.

Apparatus. The IGS method employed the gas-stripping apparatus similar to that described by Mackay and Shiu.[17] Two stripping vessels in similar size were fabricated respectively using stainless steel (SUS304) and glass (90 cm high with 5.5 cm inner diameter (i.d.)). Each setup consists of two columns fused together in the bottom. The outer column, filled with circulated water, served as a water jacket for temperature control, while the inner column was used for gas stripping measurements with four sampling ports installed at different positions.

The preparation of the aqueous solution is an important factor in IGS experiments. It is noteworthy that the existence of organic solvent in the solution might potentially affect the experimental results for FTOHs, though Ten Hulsher et al.[18] have demonstrated a negligible solvent effect on the measurement of K_H for some hydrophobic organic compounds by IGS. However, to minimize the loss of FTOHs during the chemical dissolving process and achieve complete dissolution, this study followed the similar approaches with other studies using the IGS method.[19,20] The solution was prepared using Milli-Q water in a 2 dm^3 volumetric flask and spiked with 1 cm^3 mixed standards of 4:2, 6:2, and 8:2 FTOH in methanol, equivalent to 200 μg for each compound. One cm^3 of solution containing 40 μg of 10:2 FTOH in methanol was spiked separately due to its low solubility.[21]

The flask was covered with aluminum foil and stirred with a magnetic bar for 1 day. The measured aqueous concentration of FTOHs in the flask was lower than the reported or estimated saturation level of each compound.[21] Then the solution was transferred to the vessel and allowed to sit in the thermostatted column overnight prior to gas stripping experiment to reach equilibrium with the apparatus. A nitrogen stream with a mass fraction purity of 0.999995 was used as stripping gas with an in-line mass flow controller (FMA5512, OMEGA Engineering, USA) maintaining a constant flow rate at 0.83 $cm^3 \cdot s^{-1}$. To minimize the water partitioning effect during the experiment, the nitrogen stream was saturated with water by passing through tandem 500 cm^3 gas-washing bottles before entering the column. Bubbling was carried out through an air stone with pore size in the range of (40 to 50) μm. Temperature control was done by using water jacket circulated through the outer column to maintain the isothermal conditions of the stripping system.

Both concentrations in the aqueous solution and the existing gas were monitored during each run. No statistical difference in aqueous concentrations collected from different sampling ports was discernible, indicating a homogeneous distribution of FTOHs within the vessel. Therefore, a 6 cm^3 aqueous sample was withdrawn from the middle section of the column every 0.5 h in the subsequent experiments. The FTOHs in the exiting gas stream were collected by XAD-2 sorbent tubes (OSHA versatile sampler tubes, SKC, USA) for 0.5 h during a total 3 h sampling period after an initial 1 h purging of the system. The sorbent tubes were then spiked with 50 ng of ^{13}C-8:2 FTOH in methanol prior to sampling for recovery calculation and data quality monitoring.

To investigate the adsorption of FTOHs onto different material surfaces, another set of batch experiments was conducted using 10 cm^3 vials (60 mm high with 16 mm i.d.) made by stainless steel and glass, respectively. Duplicate sets of vials were filled with 10 cm^3 aqueous solution containing 100 ng of each FTOH with minimal headspace remaining. Parallel samples were kept in a water bath under different temperatures and time durations. The aqueous solution was removed at the end of the

Table 1. Instrumental Detection Limits (IDL) and Instrumental Quantification Limits (IQL) of FTOHs Calculated Using the NIOSH Method[22]

compound	IDL/pg	IQL/pg
4:2 FTOH	1.20	3.98
6:2 FTOH	2.52	8.38
8:2 FTOH	0.88	2.96
10:2 FTOH	1.48	4.92

experiments for concentration measurements, and then the remaining FTOHs absorbed to the surfaces were recovered by MTBE. Results showed the adsorption of all FTOHs within the vial equilibrated after 6 h. Therefore, to ensure equilibrium had been reached, 8 h was chosen for the adsorption experiments.

Sample Treatment and Quality Control. For the gas samples collected in IGS, the filter with the front section of the XAD-2 resin in the sorbent tube was transferred to a 4 cm^3 vial and extracted with mixture of acetone and MTBE in equal proportions by volume. The back sections of the XAD-2 resin were also analyzed to ensure no breakthrough during the sampling period. The volume of the sample was reduced with ETOAc as a keeper to 500 mm^3 by a gentle stream of high purity nitrogen. A 10 mm^3 internal standard containing 2000 ng of 7:1 FA and 11:1 FA in ETOAc was added prior to the analysis for volume correction. For the water samples, 50 ng of ^{13}C-8:2 FTOH in methanol was spiked in before extraction. Then the aqueous samples were solvent-extracted three times with 1 cm^3 MTBE in 15 cm^3 centrifuge tubes, and the combined extracts were reduced to about 500 mm^3 in ETOAc. A 10 mm^3 internal standard was added prior to the analysis.

All glassware was baked at 673 K for 2 h before each experiment to minimize contamination. Procedural blanks were run with each batch of aqueous and gaseous samples to detect background contamination during the experimental process. All samples were extracted immediately upon collection.

Results showed that none of the target compound in the blank was higher than the detection limit. Therefore, the experimental contamination could be neglected in data analysis. The average recovery rates of ^{13}C-8:2 FTOH for 112 water and 52 air samples are (89 ± 12) % and (100 ± 13) %, respectively, indicating high credibility of the data gained in this experiment.

Instrumental Analysis. Sample quantification was conducted using an Agilent 6890N network gas chromatograph with a 5973 network mass selective detector (GC-MS) using helium as the carrier gas (0.02 $cm^3 \cdot s^{-1}$). 7:1 FA served as the internal standard for all analyses except for 10:2 FTOH, which used 11:1 FA instead. Gas inlet parameters include: inlet temperature of 513 K; 2 mm^3 splitless injection; purge flow of 0.83 $cm^3 \cdot s^{-1}$ at 60 s. Chromatographic separation of FTOHs was performed on an HP-INNOWAX column (J&W Scientific, USA, 0.25 μm film thickness, 0.25 mm i.d., 60 m). The oven temperature program was set at 323 K for 120 s, 0.05 $K \cdot s^{-1}$ to 353 K, and then 0.17 $K \cdot s^{-1}$ until 503 K with hold for 300 s.

Quantification was based on area integration of the target ion of each compound. Two more ions were picked to assist qualification of the interest compound. A National Institute for Occupational Safety and Health (NIOSH) procedure[22] was employed to determine the instrumental limit of detection (IDL) and instrumental limit of quantification (IQL) for each target compound, as indicated in Table 1.

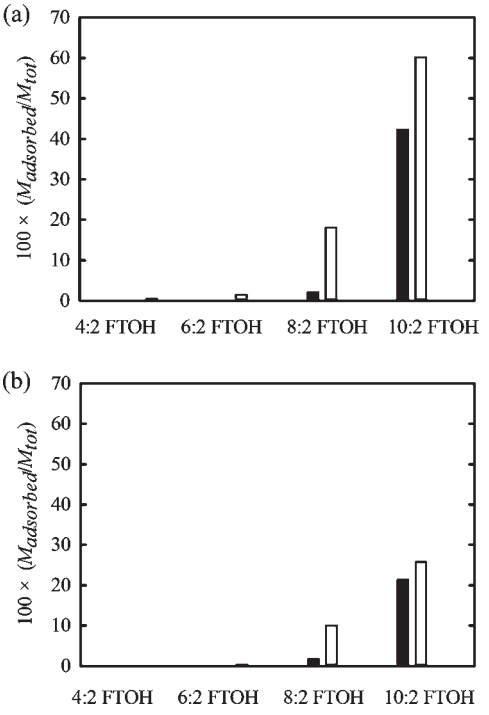

Figure 1. Adsorption ratio of FTOHs to the vial surface made of different materials. $M_{adsorbed}$, amount of FTOHs adsorbed to the vial surface; M_{tot}, total amount of FTOHs injected into the vial; ■, stainless steel; □, glass; (a) at 313 K; (b) at 323 K.

General Partitioning Models. Sparc Performs Automated Reasoning in Chemistry (SPARC) is a general purpose calculator developed by University of Georgia. It is widely used in situations where suitable measured values are not available. SPARC calculates various physicochemical parameters from molecular structure and basic environmental information. In most cases, SPARC only requires the input of simplified molecular input line entry specification (SMILES string), which is used for describing the structure of chemical molecules, to predict a parameter.

Estimation Programs Interface (EPI) Suite is another widely used software developed by United States Environmental Protection Agency to predict physicochemical properties of organic compounds. The Henrywin v3.20 integrated inside EPI Suite v4.10 is employed to estimate Henry's law constant through the group contribution and bond contribution methods.

■ RESULTS AND DISCUSSION

Adsorption of FTOHs on Glass and Stainless Steel Surface. Due to air stripping in IGS, the aqueous concentrations of FTOHs were expected to decrease with time. Preliminary results indicated a stable declining tendency of 4:2 FTOH in glass vessel. However, greater fluctuations were observed for longer-chained compounds such as 6:2 and 8:2 FTOH, while very low aqueous concentrations for the longest chain FTOH (10:2) remained constant throughout the experiment. This indicated the partitioning behaviors in glass vessel were not only governed by K_H of FTOHs but also some other factors.

Some studies investigating K_H of other hydrophobic organic compounds using the IGS method had suggested that the adsorption to glass surface might be an important factor leading to this phenomenon.[20,23] As FTOHs are also hydrophobic, it

would be possible for a certain portion of FTOHs to get adsorbed to the vessel surface as well, and the dynamic of adsorption and desorption process would further fluctuate or buffer the solution as observed in this study.

Measurements of K_H by IGS were also conducted using a stainless steel vessel. Compared with a glass vessel, the data from stainless steel showed more consistent declining trends in aqueous concentrations. To better understand the adsorption of FTOHs to the stainless steel and glass surfaces, another set of batch experiments was conducted in small glass and stainless steel vials.

Figure 1 showed the wall adsorption ratio in glass and stainless steel at 313 K (Figure 1a) and 323 K (Figure 1b). The *y* axis indicated the ratio of the amount of FTOHs recovered from the vial surface to the total amount of FTOHs injected to the vial. It can be observed that the shorter FTOHs (4:2 and 6:2) exhibited little or slight adsorption on both stainless steel and glass surfaces. In contrast, the surface adsorption increased significantly for two longer-chained FTOHs (8:2 and 10:2) on a glass surface, while stainless steel only displayed a modest adsorption for 10:2 FTOH compared with a glass surface.

The temperature was observed as another important factor, other than the fabricating material, which could also affect the wall adsorption of FTOHs, especially for longer FTOHs (8:2 and 10:2). As indicated in Figure 1, the adsorption ratio of 10:2 FTOH was reduced by half when the temperature increased from (313 to 323) K for both surfaces.

Therefore, the results of the small vial experiment provided sound evidence for the presence of surface adsorption of FTOHs, which could be an important source of fluctuating aqueous concentrations in the glass vessel discussed above.

Due to the fluctuating aqueous concentrations, no consistency was observed for calculated K_H of 6:2, 8:2, and 10:2 FTOH in IGS experiment using a glass vessel, with relative standard deviations of K_H occasionally higher than 0.5. In addition, although polypropylene (PP) was reported to be a good material for PFCs with relatively low adsorption, the temperature control in PP vessel would be an issue due to its poor thermal conductivity. Therefore, a stainless steel vessel was employed instead of the widely used glass column for K_H measurements by IGS in this study.

The loss of chemicals from the aqueous phase during IGS can also be attributed to chemical adsorbing on the air bubble surface, in addition to the chemical partitioning to air phase and chemical adsorbing to reactor wall. While the wall adsorption effect was discussed above, the air bubble surface effect was controlled by the adsorption coefficient of FTOHs on the water surface from the water side and surface-to-volume ratio of air bubbles. Upon the bursting of air bubbles, the FTOHs absorbed on gas bubble surfaces will be transferred to the headspace of the reactor and lead to the overestimation of the K_H. The detailed quantification of the influence of air bubble adsorption effect in IGS requires further study. A comparison with parallel experiments using HS and IGS with stainless steel containers might be helpful to better understand the impact of the air bubble effect.

Results of Henry's Law Constant. To measure Henry's law constant, it is essential to ensure equilibrium was achieved between gaseous and aqueous phases within the stripping vessel. Initial tests were conducted to measure the K_H values obtained at purge heights of (40, 67, and 84) cm under 323 K. Results showed that K_H values of FTOHs obtained at (67 and 84) cm yield similar values with a relative standard deviation less than 0.1, indicating that the equilibrium was reached at the height above 67 cm. To further ensure equilibrium conditions, all experiments were conservatively conducted at the height of 84 cm in this study.

Table 2. Henry's Law Constants of FTOHs Measured in This Study in the (309.6 to 334.2) K Range[a]

	T		K_H	
compound	K	K_{AW}	$Pa \cdot m^3 \cdot mol^{-1}$	log (K_H/$Pa \cdot m^3 \cdot mol^{-1}$)
4:2 FTOH	309.6	0.11 ± 0.01	283 ± 26	2.45 ± 0.04
	314.5	0.12 ± 0.01	314 ± 26	2.50 ± 0.05
	319.6	0.15 ± 0.02	399 ± 53	2.60 ± 0.05
	323	0.18 ± 0.02	483 ± 54	2.68 ± 0.05
	330	0.23 ± 0.02	631 ± 55	2.80 ± 0.04
	334.2	0.29 ± 0.01	806 ± 28	2.91 ± 0.02
6:2 FTOH	309.6	2.82 ± 0.42	7259 ± 1081	3.86 ± 0.07
	314.5	3.60 ± 0.54	9413 ± 1412	3.97 ± 0.07
	319.6	4.10 ± 0.32	10894 ± 850	4.04 ± 0.04
	323	4.27 ± 0.82	11467 ± 2202	4.06 ± 0.09
	330	4.54 ± 0.42	12456 ± 1152	4.10 ± 0.04
	334.2	5.15 ± 0.84	14309 ± 2334	4.16 ± 0.08
8:2 FTOH	309.6	2.95 ± 0.22	7593 ± 566	3.88 ± 0.03
	314.5	3.27 ± 0.54	8550 ± 1412	3.93 ± 0.08
	319.6	3.86 ± 0.22	10257 ± 585	4.01 ± 0.03
	323	4.29 ± 0.50	11520 ± 1343	4.06 ± 0.05
10:2 FTOH	309.6	3.88 ± 0.40	9987 ± 1030	4.00 ± 0.05
	314.5	4.95 ± 0.56	12943 ± 1464	4.11 ± 0.05
	319.6	5.69 ± 1.62	15119 ± 4305	4.18 ± 0.15
	323	6.03 ± 0.68	16193 ± 1826	4.21 ± 0.05
	330	6.65 ± 1.46	18245 ± 4006	4.26 ± 0.11
	334.2	7.05 ± 0.72	19589 ± 2001	4.29 ± 0.05

[a] 0.95 confidence intervals (± 2 standard deviations).[24]

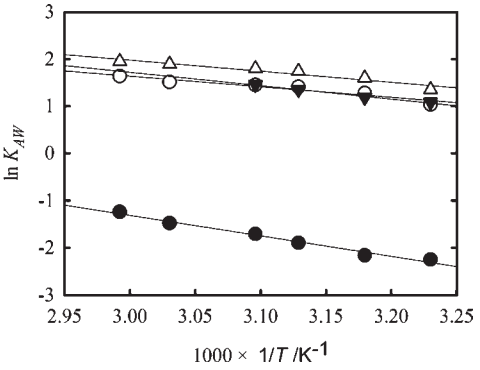

Figure 2. Measured dimensionless Henry's law constant K_{AW} of FTOHs as a function of temperature from (309.6 to 334.2) K. ●, 4:2 FTOH; ○, 6:2 FTOH; ▼, 8:2 FTOH; △, 10:2 FTOH.

Table 2 showed measured Henry's law constants of FTOHs with a confidence interval of 0.95 at each temperature. The estimates of uncertainties, with a coverage factor k = 2, were compliant with the National Institute of Standards and Technology (NIST) method of reporting.[24] All of the measured K_H values were analyzed using linear regression of ln K_{AW} versus the reciprocal of temperature to predict the K_H values (Figure 2).

Table 3. Henry's Law Constants Extrapolated to 298 K for FTOHs[a,b] along with Entropy ΔH[c] and Enthalpy ΔS[d] Obtained in This Study

	K_H	ΔH	ΔS
FTOH	$Pa \cdot m^3 \cdot mol^{-1}$	$kJ \cdot mol^{-1}$	$J \cdot K^{-1} \cdot mol^{-1}$
4:2	151 ± 27	34.6 ± 6.4	92.9 ± 19.9
6:2	5726 ± 1215	18.6 ± 7.6	69.4 ± 23.8
8:2	5039 ± 1029	23.5 ± 18.1	84.9 ± 19.6
10:2	7776 ± 1608	19.6 ± 7.4	75.2 ± 23.1

[a] Derived Henry's law constants from the linear regression analysis of measured ln K_{AW} versus the reciprocal temperature. [b] Working–Hotelling 0.95 confidence band. [c] 0.95 confidence interval ($\pm t$ critical × standard errors of the slope). [d] 0.95 confidence interval ($\pm t$ critical × standard errors of the intercept)

The r^2 values for the linear regression analysis of all FTOHs ranged from (0.92 to 0.99), validating the assumption that enthalpy ΔS and entropy ΔH were invariant over the investigated temperature range (eq 2). This finding allowed the K_H of FTOHs to be reasonably extrapolated to 298 K with estimates of uncertainties, as shown in Table 3. The calculated enthalpy ΔS and entropy ΔH of phase change based on the slope and intercept of the lines were also included in Table 3. It is noteworthy that, unlike the results obtained by Lei et al.,[15] no linear increase of both ΔS and ΔH with each additional $-CF_2-CF_2-$ unit was observed in this study. However, the extrapolated K_H of 8:2 FTOH at 298 K by Lei et al.,[15] using their ΔH and ΔS would be lower than that of 4:2 FTOH, which was inconsistent with the results reported in this study and by the other groups.[16,25]

As indicated in Table 2, the K_H values of FTOHs generally increased with the increasing fluorinated carbon chain and temperature. However, the value of K_H for 6:2 and 8:2 FTOH showed little difference. Generally speaking, if the analogue group possesses a similar structure, their K_H and molar enthalpy of phase change should increase with increasing molecular weight.[26] This trend was not observed in the current study. Similarly, Lei et al.[15] and Goss et al.[16] using HS also reported a slight reduction of K_H for 8:2 FTOH compared with 6:2 FTOH. Goss et al.[16] attributed the lower value of K_H of 8:2 FTOH to the extensive adsorption of FTOHs to the glass surface. In addition, we expect these unusual phenomena may also indicate the influence of the molecular structure of FTOHs to their physicochemical properties, since all experimental K_H data of FTOHs displayed similar trends.

It is reported that, unlike hydrocarbons, the geometry of fluorocarbons changes as the chain length increases to minimize the steric hindrance due to the larger van der Waals radius of fluorine than hydrogen. If the CF_2 units are less than eight, the fluorocarbon segments mainly form a planar and flexible zigzag conformation, while with more than eight CF_2 units, a slight distortion at each CF_2 leads to a helix conformation, which increases strongly with the increasing number of CF_2 units.[27,28] The change of molecular geometry with increasing fluorocarbon chain would impact electron density distribution within molecules and the free energy of thermodynamic process. Wang and Ober[27] reported that the melting enthalpy of a series of semifluorinated 1-bromoalkane decreased when the number of CF_2 group increased from 8 to 12.

Hydrogen bonding might also serve as another important factor. In addition to the intermolecular hydrogen bonding,

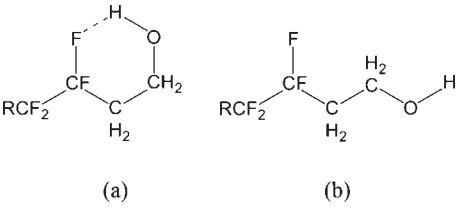

Figure 3. Molecular geometries of FTOHs. (a) Intramolecularly hydrogen bonded; (b) unbonded.

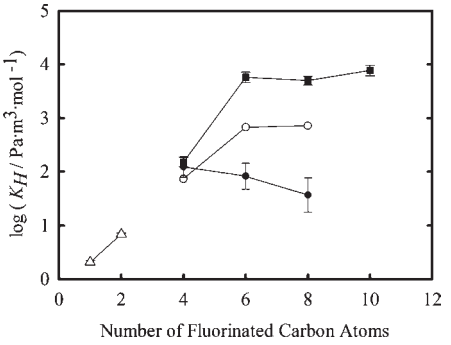

Figure 4. Plots of reported experimental Henry's law constants of FTOHs at 298 K versus the number of fluorinated carbon atoms. ■, this work using IGS; ○, Goss et al.[16] using HS; ●, Lei et al.[15] using HS; △, Chen et al.[31] using the absolute calibration method for short-chained fluorinated alcohols CF_3CH_2OH and $CF_3CF_2CH_2OH$.

multiple fluorination of alkanol also results in intramolecular hydrogen bonding within FTOHs. The X-ray crystallographic study[23] suggested a hex-shaped intramolecular bonding with hydrocarbon functional group of FTOHs at the end of the carbon chain folding back on top of fluorinated portion, as illustrated in Figure 3. The competition between intramolecular and intermolecular hydrogen bonding would affect relative physicochemical properties of FTOHs.

This hex-cyclic intramolecular hydrogen bonding and intermolecular hydrogen bonding in FTOHs, coupled with the twisting and stiffening effect of carbon segments discussed above, might further complicated the physicochemical properties, especially for longer-chained compounds such as 8:2 and 10:2 FTOH. Furthermore, all of these factors could interactively influence one another. For example, as the gradually twisted and stiffened fluorocarbon segment tends to become poorly compatible with the flexible hydrocarbon tail with increasing hydrophobic carbon chain length, the polarization of the −OH functional group was enhanced. Consequently, the hydrogen segment of longer FTOHs would be easier to establish intermolecular hydrogen bonding with other FTOHs or water molecules in aqueous phase. This could compensate the effects resulting from increasing chain length, making the longer FTOHs less volatile than expected. This effect can be illustrated as the observed vapor pressures of FTOHs were much higher than their hydrocarbon counterparts, which was believed mainly due to the masking of −OH functional group by intramolecular hydrogen bonding.[15,25,29] The K_H values of FTOHs are also approximately 1 to 2 orders of magnitude higher than those of nonsubtituted alcohols.[30]

Therefore, the slight difference of the K_H value between 6:2, 8:2, and 10:2 FTOH in this study might be due to the combined effects of conformation change and hydrogen bonding as discussed

Table 4. Henry's Law Constants of FTOHs at 298 K Generated in This Study (IGS)[a] and Calculated from Vapor Pressure (P) and Solubility (S),[b] as well as Values Predicted by Modeling Software (EPI Suite and SPARC)

	log (K_H/Pa·m^3·mol^{-1})				
compound	IGS (current study)	P/S	EPI Suite v4.10 Bond method	EPI Suite v4.10 Group method	SPARC Sep, 2009
4:2 FTOH	2.18 ± 0.09	1.77	2.74	3.23	1.02
6:2 FTOH	3.76 ± 0.10	2.54	4.18	5.23	2.4
8:2 FTOH	3.70 ± 0.08	4.10	5.62	7.23	4.31
10:2 FTOH	3.89 ± 0.10	4.01	7.06	9.23	6.71

[a] Working−Hotelling 0.95 confidence band for linearly derived Henry's law constants. [b] 4:2 FTOH: 216 Pa,[25] $3.69 \cdot 10^{-3}$ mol·kg^{-1};[21] 6:2 FTOH: 18 Pa,[25] $5.16 \cdot 10^{-5}$ mol·kg^{-1};[21] 8:2 FTOH: 4 Pa,[25] $3.19 \cdot 10^{-7}$ mol·kg^{-1};[9,32,33] 10:2 FTOH: 0.2 Pa,[25] $1.95 \cdot 10^{-8}$ mol·kg^{-1}.[21]

above, making their physicochemical properties quite different from those of their hydrocarbon counterparts.

Comparison between Experimental and Modeling Results. Plots of extrapolated experimental K_H of FTOHs at 298 K from various studies via different experimental approaches versus number of fluorinated carbon atoms were illustrated in Figure 4, including values obtained by current study using the IGS method, Goss et al.[16] and Lei et al.[15] using the HS method, as well as values of short-chained fluorinated alcohols CF_3CH_2OH and $CF_3CF_2CH_2OH$ reported by Chen et al.[31] using the absolute calibration method. It could be seen that K_H values were mainly influenced by the number of fluorinated carbon atoms except the reversed trend reported by Lei et al.,[15] which might be erroneous. It was also clear that all extrapolated values of log K_H of FTOHs by the HS method are lower than those by the IGS method. This discrepancy might be mainly attributed to the different extent of surface adsorption of FTOHs to the wall due to different surface-to-volume ratios and fabrication materials in IGS and HS. The equilibrium between bulk phase (water, air) and vessel surface in the closed container of the HS method would lead to the reduction in sampled gaseous concentration. This has been confirmed by Goss et al.,[16] who reported a slightly higher K_H value of 8:2 FTOH by using silanized glass vial. IGS, which employs a much larger vessel than HS, will suffer less from the interface adsorption effect due to the relatively lower surface-to-volume ratio.

Table 4 lists the values of log K_H at 298 K obtained in this study, calculated from vapor pressure (P) and water solubility (S),[21,25] and modeling results generated by the latest versions of EPI and SPARC (EPI Suite v4.10 and SPARC Sep, 2009). It is clear that the estimated partition coefficients by EPI and SPARC differ considerably. Through the comparison with experimental values, the group method of EPI suite v4.10 is probably not a suitable method for predicting the partitioning behavior of FTOHs as it overestimates the value by up to 6 orders of magnitude. In contrast, the EPI bond method performed relatively better but still reported higher K_H values for longer-chained FTOHs by up to 4 orders of magnitude. Compared with EPI Suite, the latest SPARC gave a closer estimation for all FTOHs except 10:2 FTOH.

To sum up, significant discrepancies were observed between experimental values and modeling predictions, which was in accordance with our expectations. Both SPARC and EPI Suite require only the input of basic structure of molecule to predict a parameter, resulting in a large uncertainty in their prediction due to lack of compensation for the geometrical features of FTOHs. The existence of cyclic intramolecular hydrogen bonding and conformation distortion also led to the conclusion that all physicochemical properties of FTOHs governed by molecular geometry will be significantly affected, as the novel geometry will impact the electron density distribution and free energy of thermodynamic process. Furthermore, the changes of the molecule's geometry with increasing chain length of FTOHs would result in difficulty in the prediction of these properties, based on differences between experimental and modeling values observed in this study.

CONCLUSIONS

The Henry's law constants of 4:2, 6:2, 8:2, and 10:2 FTOH were determined using the IGS method at various temperatures from (309.6 to 334.2) K. Results showed great fluctuation in calculated K_H values in IGS employing a glass vessel, especially for FTOHs with longer fluorocarbon chains. In contrast, a set of stable K_H values was observed by stainless steel vessel. The adsorption of FTOHs to vessel surface was suspected to be the main influencing factor for this phenomenon and was investigated by a batch experiment employing stainless steel and glass vials. A significantly stronger adsorption of long-chained FTOHs, 8:2 and 10:2, to the glass than stainless steel surface was observed. Furthermore, unlike their hydrocarbon counterparts, no linear increase of K_H for FTOHs was observed in this study, which was consistent with the results by other researchers using the HS approach. The unique geometry of FTOHs with hydrogen bonding and conformation distortion was believed to contribute to the unusual physicochemical properties of FTOHs reported in experiments. It also increased the difficulties in prediction by modeling software such as SPARC and EPI Suite. In addition, variations of deviations between IGS-generated and HS-generated values for different FTOHs were observed, which might be mainly attributed to the differences in surface adsorption of FTOHs due to different surface-to-volume ratios and fabrication materials in IGS and HS methods.

AUTHOR INFORMATION

Corresponding Author

*E-mail: wcchang@ntu.edu.sg (V.W.-C.C.). Tel.: +65 6790 4773. Fax: +65 6792 1650.

Notes

†E-mail: wu0009ng@e.ntu.edu.sg (Y.W.).

REFERENCES

(1) Prevedouros, K.; Cousins, I. T.; Buck, R. C.; Korzeniowski, S. H. Sources, fate and transport of perfluorocarboxylates. *Environ. Sci. Technol.* **2006**, *40*, 32–44.

(2) Washburn, S. T.; Bingman, T. S.; Braithwaite, S. K.; Buck, R. C.; Buxton, L. W.; Clewell, H. J.; Haroun, L. A.; Kester, J. E.; Rickard, R. W.; Shipp, A. M. Exposure assessment and risk characterization for perfluorooctanoate in selected consumer articles. *Environ. Sci. Technol.* **2005**, *39*, 3904–3910.

(3) Dapremont-avignon, C.; Calas, P.; Commeyras, A.; Amatore, C. Synthesis of perfluoroalkyl carboxylic acids by reaction of perfluoroalkyl

iodides with electrogenerated superoxide ion. *J. Fluorine Chem.* **1991**, *51*, 357–379.

(4) Dreyer, A.; Ebinghaus, R. Polyfluorinated compounds in ambient air from ship- and land-based measurements in northern Germany. *Atmos. Environ.* **2009**, *43*, 1527–1535.

(5) Stock, N. L.; Lau, F. K.; Ellis, D. A.; Martin, J. W.; Muir, D. C. G.; Mabury, S. A. Polyfluorinated Telomer Alcohols and Sulfonamides in the North American Troposphere. *Environ. Sci. Technol.* **2004**, *38*, 991–996.

(6) Jahnke, A.; Huber, S.; Temme, C.; Kylin, H.; Berger, U. Development and application of a simplified sampling method for volatile polyfluorinated alkyl substances in indoor and environmental air. *J. Chromatogr., A* **2007**, *1164*, 1–9.

(7) Ellis, D. A.; Martin, J. W.; De Silva, A. O.; Mabury, S. A.; Hurley, M. D.; Sulbaek Andersen, M. P.; Wallington, T. J. Degradation of fluorotelomer alcohols: A likely atmospheric source of perfluorinated carboxylic acids. *Environ. Sci. Technol.* **2004**, *38*, 3316–3321.

(8) Nakayama, K.; Iwata, H.; Tao, L.; Kannan, K.; Imoto, M.; Kim, E. Y.; Tashiro, K.; Tanabe, S. Potential effects of perfluorinated compounds in common cormorants from Lake Biwa, Japan: An implication from the hepatic gene expression profiles by microarray. *Environ. Toxicol. Chem.* **2008**, *27*, 2378–2386.

(9) Ellis, D. A.; Martin, J. W.; Mabury, S. A.; Hurley, M. D.; Sulbaek Andersen, M. P.; Wallington, T. J. Atmospheric lifetime of fluorotelomer alcohols. *Environ. Sci. Technol.* **2003**, *37*, 3816–3820.

(10) Brutseart, W.; Jirka, G. H. *Gas transfer at water surfaces*; Springer: Hingham, 1984.

(11) Shoeib, M.; Harner, T.; Vlahos, P. Perfluorinated chemicals in the arctic atmosphere. *Environ. Sci. Technol.* **2006**, *40*, 7577–7583.

(12) Renner, R. Leftovers may explain perfluorinated compound puzzle. *Environ. Sci. Technol.* **2006**, *40*, 1376–1377.

(13) Jahnke, A.; Ahrens, L.; Ebinghaus, R.; Temme, C. Urban versus remote air concentrations of fluorotelomer alcohols and other polyfluorinated alkyl substances in Germany. *Environ. Sci. Technol.* **2007**, *41*, 745–752.

(14) Arp, H. P. H.; Niederer, C.; Goss, K. U. Predicting the partitioning behavior of various highly fluorinated compounds. *Environ. Sci. Technol.* **2006**, *40*, 7298–7304.

(15) Lei, Y. D.; Wania, F.; Mathers, D.; Mabury, S. A. Determination of vapor pressures, octanol-air, and water-air partition coefficients for polyfluorinated sulfonamide, sulfonamidoethanols, and telomer alcohols. *J. Chem. Eng. Data* **2004**, *49*, 1013–1022.

(16) Goss, K. U.; Bronner, G.; Harner, T.; Hertel, M.; Schmidt, T. C. The partition behavior of fluorotelomer alcohols and olefins. *Environ. Sci. Technol.* **2006**, *40*, 3572–3577.

(17) Mackay, D.; Shiu, W. Y. A critical review of Henry's law constants for chemicals of environmental interest. *J. Phys. Chem. Ref. Data* **1981**, *10*, 1175–1225.

(18) Ten Hulscher, T. E. M.; Van der Velde, L. E.; Bruggeman, W. A. Temperature dependence of Henry's law constants for selected chlorobenzenes, polychlorinated biphenyls and polycyclic aromatic hydrocarbons. *Environ. Toxicol. Chem.* **1992**, *11*, 1595–1603.

(19) Miyano, Y.; Ashimori, S.; Otuka, T.; Dairaku, T.; Kitamoto, T.; Kume, Y.; Tateishi, Y.; Nishiguchi, Y.; Miura, R.; Mitani, T. Henry's law constants and infinite dilution activity coefficients of propane, propene, butane, 2-methylpropane, 1-butene, 2-methylpropene, trans-2-butene, cis-2-butene, 1,3-butadiene, dimethyl ether, chloroethane, and 1,1-difluoroethane in 2-methylphenol, 3-methylphenol, and 4-methylphenol. *J. Chem. Eng. Data* **2010**, *55*, 4956–4960.

(20) Bamford, H. A.; Poster, D. L.; Baker, J. E. Henry's law constants of polychlorinated biphenyl congeners and their variation with temperature. *J. Chem. Eng. Data* **2000**, *45*, 1069–1074.

(21) Liu, J.; Lee, L. S. Effect of fluorotelomer alcohol chain length on aqueous solubility and sorption by soils. *Environ. Sci. Technol.* **2007**, *41*, 5357–5362.

(22) Kennedy, E. R.; Fischbach, T. J.; Song, R.; Eller, P. M.; Shulman, S. A. *Guidelines for Air Sampling and Analytical Method Development and Evaluation*; DHHS (NIOSH) Publication 95−117; U.S. Department of Health and Human Services: Cincinnati, OH, 1995.

(23) Bamford, H. A.; Poster, D. L.; Baker, J. E. Temperature dependence of Henry's law constants of thirteen polycyclic aromatic hydrocarbons between 4 °C and 31 °C. *Environ. Toxicol. Chem.* **1999**, *18*, 1905–1912.

(24) Taylor, B. N.; Kuyatt, C. E. *Guidelines for Evaluating and Expressing the Uncertainty of NIST Measurement Results*; NIST Technical Note 1297; U.S. Department of Commerce Technology Administration: Gaithersburg, MD, 1994.

(25) Krusic, P. J.; Marchione, A. A.; Davidson, F.; Kaiser, M. A.; Kao, C. P. C.; Richardson, R. E.; Botelho, M.; Waterland, R. L.; Buck, R. C. Vapor pressure and intramolecular hydrogen bonding in fluorotelomer alcohols. *J. Phys. Chem. A* **2005**, *109*, 6232–6241.

(26) Ong, S. K.; Lion, L. W. Effects of soil properties and moisture on the sorption of trichloroethylene vapor. *Water Res.* **1991**, *25*, 29–36.

(27) Wang, J.; Ober, C. K. Solid state crystalline and liquid crystalline structure of semifluorinated 1-bromoalkane compounds. *Liq. Cryst.* **1999**, *26*, 637–648.

(28) Bunn, C. W.; Howells, E. R. Structures of molecules and crystals of fluoro-carbons. *Nature* **1954**, *174*, 549–551.

(29) Stock, N. L.; Ellis, D. A.; Deleebeeck, L.; Muir, D. C. G.; Mabury, S. A. Vapor Pressures of the Fluorinated Telomer Alcohols - Limitations of Estimation Methods. *Environ. Sci. Technol.* **2004**, *38*, 1693–1699.

(30) Mackay, D. S.; Shiu, W. Y.; Kuo, C. M. *Illustrated handbook of physical-chemical properties and environmental fate for organic chemicals*; Lewis: Boca Raton, FL, 1993.

(31) Chen, L.; Takenaka, N.; Bandow, H.; Maeda, Y. Henry's law constants for C2-C3 fluorinated alcohols and their wet deposition in the atmosphere. *Atmos. Environ.* **2003**, *37*, 4817–4822.

(32) Liu, J.; Lee, L. S. Solubility and sorption by soils of 8:2 fluorotelomer alcohol in water and cosolvent systems. *Environ. Sci. Technol.* **2005**, *39*, 7535–7540.

(33) Kaiser, M. A.; Cobranchi, D. P.; Kao, C. P. C.; Krusic, P. J.; Marchione, A. A.; Buck, R. C. Physicochemical properties of 8−2 fluorinated telomer B alcohol. *J. Chem. Eng. Data* **2004**, *49*, 912–916.